FACTA UNIVERSITATIS
Series: **Mechanical Engineering** Vol. 12, N° 3, 2014, pp. 261 - 276

Original scientific paper

THE CRITICAL LOAD PARAMETER OF A TIMOSHENKO BEAM WITH ONE-STEP CHANGE IN CROSS SECTION

UDC 534.1

Goran Janevski[1], Marija Stamenković[2], Mariana Seabra[3]

[1]University of Niš, Department of Mechanical Engineering, Serbia
[2]Mathematical Institute of the SASA, Belgrade, Serbia
[3]University of Porto, Faculty of Engineering – FEUP, Portugal

Abstract. *The paper analyzes the transverse vibration of a Timoshenko beam with one-step change in cross-section when subjected to an axial force. The axial force is equal in both of the beam portions. Three types of beam which occur commonly in engineering application are considered. The frequency equation of the Timoshenko beam with one-step change in cross-section is expressed as the fourth order determinant equated to zero. The critical compressive axial force is expressed as a function of the critical load parameter which is tabulated for four classical boundary conditions. Apart from the results presented in Tables, the paper also provides calculated values of the critical load parameter for other values of system parameters along with the graphic representation of their dependence on the step position parameter.*

Key Words: *Timoshenko Beam, Frequency Equation, Critical Axial Load, Critical Load Parameter, One-step Beam*

1. INTRODUCTION

Mechanical and other engineering structures often contain beams with step changes in cross-section. Stepped beams are increasingly used in many fields of engineering and practically always as structural elements. Due to the frequent application, they can be very different structures, subjected to various types of loads. For this reason, their dynamic properties have been investigated by many authors.

Among the first ones are Jang and Bert [1-2] who have given the first exact results for natural frequencies of a stepped beam. In Jang and Bert's paper [1] the exact solution for fundamental natural frequencies is compared with the results obtained by the use of the finite element method. In the next paper by the same authors [2] higher mode frequencies of a

Received October 10, 2014 / Accepted November 19, 2014
Corresponding author: Goran Janevski
University of Niš, Department of Mechanical Engineering,
Serbia E-mail: gocky.jane@gmail.com

stepped beam are obtained, expressing the frequency equation as the fourth-order determinant equated to zero.

The vibration of Euler-Bernoulli beam with step changes in cross-section and under axial forces is considered by Naguleswaran [2-7]. The author presents the first three frequencies and the first two critical axial forces for beams with several combinations of axial forces in two portions, and for 16 sets of boundary combinations and three types which occur commonly in engineering applications. Also, Naguleswaran [6] investigates the sensitivity of frequency parameters from the step location factor and the "active" dimension factor. The sensitivity is presented for the selected system parameters. The vibration of an Euler-Bernoulli beam with three step changes and elastic end supports is investigated in [7]. The first three frequency parameters are tabulated for the selected sets of system parameters and classical end support and 35 types of elastic end supports. Vibration and stability of Euler-Bernoulli tie-bars are considered by Naguleswaran [3]. The first three frequency parameters and the first two buckling axial forces are tabulated for three type arrangements with different number of rings and various end supports. The frequencies, in graphical form, of a uniform Euler-Bernoulli beam under constant axial compressive and tensile force for the classical boundary conditions are presented by Bokaian [8-9].

By means of the Adomian decomposition method, Mao and Pietrzko [10] investigate the free vibrations of a stepped beam. The first four natural frequencies for classical end supports are tabulated. Also, the authors obtain the frequencies for the stepped beam with a translational and rotational spring at one and both ends. Their results are compared with those obtained in [7]. Mao [11] has extended the study in [10] to multiple-stepped beams and compared them with those obtained in [3].

By using the continuous-mass transfer matrix method, Wu and Chang [12] have investigated free vibration of the axial loaded multi-step Timoshenko non-uniform beam carrying any number of concentrated elements. In this paper the authors take into consideration the effects of shear deformation, rotary inertia and their joint action term, and thus determine the exact natural frequencies. Zhang at al. [13] have developed an analytic method to study transverse vibrations of double-beam systems, in which two parallel Timoshenko beams are connected by discrete springs and coupled with various discontinuities. By dividing the entire structure into a series of distinct components, and then systematically organizing compatibility and boundary conditions with matrix formulations, closed-form expressions for the exact natural frequencies, mode shapes and frequency response functions can be determined. Parametric studies are performed for a practical example to illustrate the influences of the parametric variabilities on the dynamic behaviors.

In the present paper, the emphasis is on the critical axial force and natural frequencies of a Timoshenko stepped beam. The three types of frequent use in engineering applications are considered. The frequency equations for four combinations of the classical boundary conditions are expressed as the second order determinants equated to zero. The critical axial force is presented in the function of the dimensionless parameter. The influence of a flexural rigidity ratio, slenderness ratio and type of beam are considered. The obtained results are displayed graphically for a set of combinations of dimension factors and location parameters.

2. Problem Formulation

The basic differential equations of motion for the analysis will be reduced by considering the Timoshenko-beam of length *L*, subjected to axial compressive force *F*. This will be applied on the basis of the following assumptions:

- The behavior of the beam material is linear elastic,
- The cross-section is rigid and constant throughout the length of the beam and has one plane of symmetry,
- Shear deformations of the cross-section of the beam are taken into account while the elastic axial deformations are ignored,
- The equations are derived bearing in mind the geometric axial deformations, and,
- Axial forces F acting on the ends of the beam do not change with time.

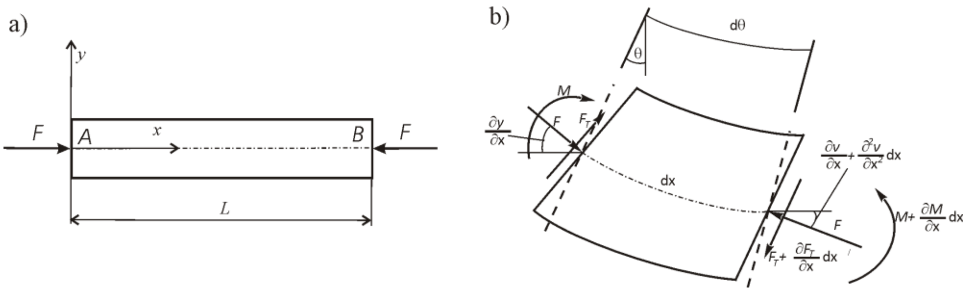

Fig. 1 The coordinate system and notation for the beam: a) Timoshenko-beam subjected to an axial compressive force F ; b) Deflected differential beam element of length dx

A beams element of length *dx* between two cross-sections taken normal to the deflected axis of the beam is shown in Fig. 1b. Since the slope of the beam is small, the normal forces acting on the sides of the element can be taken as equal to axial compressive force *F*. Shearing force F_T is related to the following relationship:

$$F_T = kGA\left(\frac{\partial v}{\partial x} - \psi\right) \tag{1}$$

where $v = v(x,t)$ is the displacement of the cross-section in *y*-direction, $\partial v/\partial x$ is the global rotation of the cross section, $\psi = \psi(x,t)$ is the bending rotation, *G* is the shear modulus, *A* is the area of the beam cross-section, and *k* is the shear correction factor of cross-section. Analogously, the relationship between bending moment *M* and bending angles ψ is given by:

$$M = -EI_z \frac{\partial \psi}{\partial x} \tag{2}$$

where *E* is the Young's modulus and I_z is the second moment of the area of the cross-section. Finally, forces and moments of inertia are given by:

$$f = -\rho A \frac{\partial^2 w}{\partial t^2}\ ,\ J = -\rho I_z \frac{\partial^2}{\partial t^2}\ , \tag{3}$$

respectively, where ρ is the mass density. The dynamic-forces equilibrium conditions of these forces are given by the following equations:

$$m\frac{\partial^2 v}{\partial t^2} - kGA\left(\frac{\partial^2 v}{\partial x^2} - \frac{\partial \psi}{\partial x}\right) + F\frac{\partial^2 v}{\partial x^2} = 0 \tag{4}$$

$$I\frac{\partial^2 \psi}{\partial t^2} - kGA\left(\frac{\partial v}{\partial x} - \psi\right) - K\frac{\partial^2 \psi}{\partial x^2} = 0 \tag{5}$$

where $m = \rho A$ is the mass per unit length and $K = EI_z$ is the flexural rigidity. The equations on motion (4-5), which are coupled together, are reduced by standard procedure, eliminating ψ, to the following fourth-order partial differential equation:

$$K\left(1 - \frac{F}{kGA}\right)\frac{\partial^4 v}{\partial x^4} + F\frac{\partial^2 v}{\partial x^2} + I_z\left(\frac{F}{kGA} - \frac{E}{kG} - 1\right)\frac{\partial^4 v}{\partial x^2 \partial t^2} + m\frac{\partial^2 v}{\partial t^2} + \frac{I_z}{kG}\frac{\partial^4 v}{\partial t^4} = 0 \tag{6}$$

3. The Frequency Equation of the Stepped Beam

In this section of the paper a general theory for the determination of the natural frequencies and the critical buckling load of a beam with step change in cross-section is given. Ends A and B are on classical clamped (*cl*), pinned (*pn*) and free (*fr*) supports. Each beam portion is made of some material with Young's modulus E and mass density ρ, and has a cross-section with a uniform cross-section of area A_i and moment inertia I_i. The flexural rigidity, mass per unit length and the length of the beam portion are K_i, m_i and L_i. The axial force in beam portion is F_i. The coordinate systems with origin at A and B are in opposite directions.

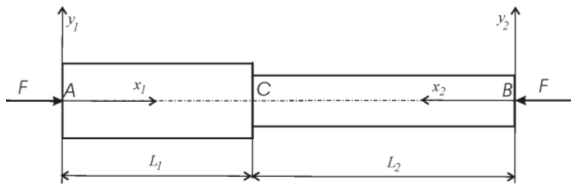

Fig. 2 The coordinate system and notation for the stepped beam

The dynamics of each beam portion are treated separately. If we apply the above-mentioned procedure to a differential element of each beam portion, the following set of coupled differential equations will be obtained:

$$EI_1\left(1 - \frac{F}{kGA_1}\right)\frac{\partial^4 v_1}{\partial x_1^{\,4}} + F\frac{\partial^2 v_1}{\partial x_1^{\,2}} + I_1\left(\frac{F}{kGA_1} - \frac{E}{kG} - 1\right)\frac{\partial^4 v_1}{\partial x_1^{\,2}\partial t^2} + m_1\frac{\partial^2 v_1}{\partial t^2} + \frac{I_1}{kG}\frac{\partial^4 v_1}{\partial t^4} = 0 \tag{7}$$

$$EI_2\left(1 - \frac{F}{kGA_2}\right)\frac{\partial^4 v_2}{\partial x_2^{\,4}} + F\frac{\partial^2 v_2}{\partial x_2^{\,2}} + I_2\left(\frac{F}{kGA_2} - \frac{E}{kG} - 1\right)\frac{\partial^4 v_2}{\partial x_2^{\,2}\partial t^2} + m_2\frac{\partial^2 v_2}{\partial t^2} + \frac{I_2}{kG}\frac{\partial^4 v_2}{\partial t^4} = 0 \tag{8}$$

The standard approach to solving Eqs. (7, 8) is by separating the variables, and the same procedure may be applied here. Thus, assuming that:

$$v_i(x_i,t) = y_i(x_i)T(t),\ i = 1,2, \tag{9}$$

where $y_i(x_i)$, are the known mode shape functions which will be determined on the basis of the type of beam supports. Assuming time harmonic motion, the unknown time function can be assumed to have the following form:

$$T(t) = e^{j\omega t},\ j = \sqrt{-1}\ , \tag{10}$$

where ω denotes the circular natural frequency of the system. To express the set of Eqs. (7-8) in the dimensionless form one defines dimensionless abscissas X_i, amplitude Y_i and step position parameter R_i as follows:

$$X_i = \frac{x_i}{L},\ \ Y_i = \frac{y_i}{L},\ \ R_i = \frac{L_i}{L},\ i = 1,2, \tag{11}$$

Also, adopt the "reference beam" with the following characteristics: area of the beam cross-section A_R, length L, mass per unit m_R and flexural rigidity EI_R. Then we can define dimensionless flexural rigidity ratio θ_i, mass per unit ratio μ_i and dimensionless axial force τ in the form:

$$\theta_i = \frac{EI_i}{EI_R},\ \ \mu_i = \frac{m_i}{m_R},\ \ \tau = \frac{FL^2}{EI_R},\ i = 1,2. \tag{12}$$

Introducing the general solutions (9) into Eqs. (7-8), considering dimensionless values, one gets the system of dimensionless differential equations:

$$\theta_i\left(1-\delta_R\frac{\chi}{k}\frac{\tau}{\mu_i}\right)\frac{d^4Y_i(X_i)}{dX_i^4}+\left\{\tau+\delta_R^4\delta_{Ri}\left[1+\frac{\chi}{k}\left(1-\delta_R\frac{\tau}{\mu_i}\right)\right]\right\}\frac{d^2Y_i(X_i)}{dX_i^2}$$
$$-\mu_i\alpha_R^4\left(1-\frac{\chi}{k}\frac{\theta_i}{\mu_i}\delta_R^2\alpha_R^4\right)Y_i(X_i)=0\ , \tag{13}$$

where $\chi = \dfrac{E}{G} = 2.6$.

In Eq. (13) α_R is the natural frequency parameter and δ_R is the slenderness ratio of the beam:

$$\alpha_R^4 = \frac{m_R L^4}{EI_R}\omega^2\ \ ,\ \ \delta_R = \frac{I_R}{A_R L^2} = \left(\frac{i_R}{L}\right)^2, \tag{14}$$

where i_R is the radius of gyration of the reference beam.

The solutions of Eq. (13) are assumed to be:

$$Y_i(X_i) = A_i e^{(u_i X_i)},\ \ i = 1,2. \tag{15}$$

For the non-trivial solution, we can determine u_i as the solution of the characteristic equation in the form:

$$u_i = \pm\sqrt{\frac{-\Delta_{2i}\pm\sqrt{\Delta_{2i}^2-4\Delta_{4i}\Delta_{0i}}}{2\Delta_{4i}}},\ i = 1,2, \tag{16}$$

where:

$$\Delta_{4i}=\theta_i\left(1-\delta_R\frac{\chi}{k}\frac{\tau}{\mu_i}\right),\ \Delta_{2i}=\tau+\alpha_R^4\delta_R\theta_i\left[1+\frac{\chi}{k}\left(1-\delta_R\frac{\tau}{\mu_i}\right)\right], \quad \Delta_{0i}=-\mu_i\alpha_R^4\left(1-\frac{\chi}{k}\frac{\theta_i}{\mu_i}\delta_R^2\alpha_R^4\right). \tag{17}$$

With the use of Euler's formula, solution (15) can be written as:

$$Y_i(X_i)=C_{1,i}\cosh(a_iX_i)+C_{2,i}\sinh(a_iX_i)+C_{3,i}\cosh(b_iX_i)+C_{4,i}\sinh(b_iX_i), \tag{18}$$

where $C_{j,i}$ (i = 1,2, j = 1,2,3,4) are eight constants to be determined from the initial conditions and:

$$a_i=\sqrt{\frac{-\Delta_{2i}+\sqrt{\Delta_{2i}^2-4\Delta_{4i}\Delta_{0i}}}{2\Delta_{4i}}},\ b_i=\sqrt{\frac{-\Delta_{2i}-\sqrt{\Delta_{2i}^2-4\Delta_{4i}\Delta_{0i}}}{2\Delta_{4i}}}\quad i=1,2. \tag{19}$$

The need for Eq. (18) to satisfy the boundary conditions at A and B may be used to eliminate four of the constants. The mode shape of the beam portions may be expressed as:

$$Y_i(X_i)=A_{i1}U_{i1}(X_i)+A_{i2}U_{i2}(X_i),\ \ i=1,2. \tag{20}$$

where A_{i1} and A_{i2} are unknown constants and functions $U_{i1}(X_i)$ and $U_{i2}(X_i)$ for the classical boundary conditions are:

For clamped,

$$U_{i1}(X_i)=\cosh(a_iX_i)-\cosh(b_iX_i),$$
$$U_{i2}(X_i)=\sinh(a_iX_i)-\frac{a_i}{b_i}\sinh(b_iX_i).$$

For pinned,

$$U_{i1}(X_i)=\sinh(a_iX_i),\ U_{i2}(X_i)=\sinh(b_iX_i). \tag{21}$$

for free,

$$U_{i1}(X_i)=\cosh(a_iX_i)-\left(\frac{a_i}{b_i}\right)^2\cosh(b_iX_i),$$
$$U_{i2}(X_i)=\sinh(a_iX_i)-\frac{\theta_ia_i^3+\tau a_i}{\theta_ib_i^3+\tau b_i}\sinh(b_iX_i).$$

Taking into account the opposite direction coordinate axes at A and B, the need to satisfy the continuity of deflection and the slope and compatibility of bending moment and shearing force at C will result in the following equations:

$$Y_1(R_1)=Y_1(R_2),\ \frac{dY_1(R_1)}{dX_1}=-\frac{dY_2(R_2)}{dX_2}, \tag{22}$$

$$\theta_1\frac{d^2Y_1(X_1)}{dX_1^2}=\theta_2\frac{d^2Y_2(X_2)}{dX_2^2},\ \theta_1\frac{d^3Y_1(X_1)}{dX_1^3}+\tau\frac{dY_1(R_1)}{dX_1}=-\left(\theta_2\frac{d^3Y_2(X_2)}{dX_2^3}+\tau\frac{dY_2(R_2)}{dX_2}\right).$$

Substituting the solution (20) into Eq. (22) and rewriting in the matrix form, one obtains the following homogenous set of four algebraic equations:

$$\begin{bmatrix} u_{11}(R_1) & u_{12}(R_1) & -u_{21}(R_2) & -u_{22}(R_2) \\ \dfrac{du_{11}(R_1)}{dX_1} & \dfrac{du_{12}(R_1)}{dX_1} & \dfrac{du_{21}(R_2)}{dX_2} & \dfrac{du_{22}(R_2)}{dX_2} \\ \theta_1 \dfrac{d^2u_{11}(R_1)}{dX_1^2} & \theta_1 \dfrac{d^2u_{12}(R_1)}{dX_1^2} & -\theta_2 \dfrac{d^2u_{21}(R_2)}{dX_2^2} & -\theta_2 \dfrac{d^2u_{22}(R_2)}{dX_2^2} \\ B_{11}(R_1) & B_{12}(R_1) & B_{21}(R_2) & B_{22}(R_2) \end{bmatrix} \begin{Bmatrix} A_{11} \\ A_{12} \\ A_{21} \\ A_{22} \end{Bmatrix} = \begin{Bmatrix} 0 \\ 0 \\ 0 \\ 0 \end{Bmatrix}, \tag{23}$$

where:

$$B_{mn}\left(R_m\right) = \theta_m \frac{d^3u_{mn}(R_m)}{dX_m^3} + \tau \frac{du_{mn}(R_m)}{dX_m}. \tag{24}$$

For the non-trivial solution, the coefficient matrix must be singular, one gets the frequency equation:

$$\begin{vmatrix} u_{11}(R_1) & u_{12}(R_1) & -u_{21}(R_2) & -u_{22}(R_2) \\ \dfrac{du_{11}(R_1)}{dX_1} & \dfrac{du_{12}(R_1)}{dX_1} & \dfrac{du_{21}(R_2)}{dX_2} & \dfrac{du_{22}(R_2)}{dX_2} \\ \theta_1 \dfrac{d^2u_{11}(R_1)}{dX_1^2} & \theta_1 \dfrac{d^2u_{12}(R_1)}{dX_1^2} & -\theta_2 \dfrac{d^2u_{21}(R_2)}{dX_2^2} & -\theta_2 \dfrac{d^2u_{22}(R_2)}{dX_2^2} \\ B_{11}(R_1) & B_{12}(R_1) & B_{21}(R_2) & B_{22}(R_2) \end{vmatrix} = 0. \tag{25}$$

4. Critical Axial Force, Critical Load Parameter

Of all the modes of failure, buckling is probably the most common and most catastrophic one. For this reason, the critical buckling load is an important characteristic of a mechanical structure. As it is known, the critical buckling load for uniform beam is:

$$\tau_{cr,u} = \left(\frac{\pi}{k_r}\right)^2, \tag{26}$$

where k_r depends on the boundary conditions and one has

- $k_r = 1$ for pinned/pinned beam
- $k_r = 1/2$ for clamped/clamped beam
- $k_r = 2$ for clamped/free beam
- $k_r = 0.69915566$ for clamped/pinned beam.

In order to verify the proposed method for the analysis of the vibration of the stepped beam, several numerical examples with different boundary conditions, step positions, slenderness ratio and moment of inertia parameter will be discussed in this section. Assuming that the stepped beam has a uniform Young's modulus E and density ρ, the present paper considers three of the types which occur commonly in engineering application. The first two are beams of a rectangular cross-section with step changes in breadth and depth and constant depth and breadth, respectively. The third type of beam has a circular cross-section with the step change in diameter.

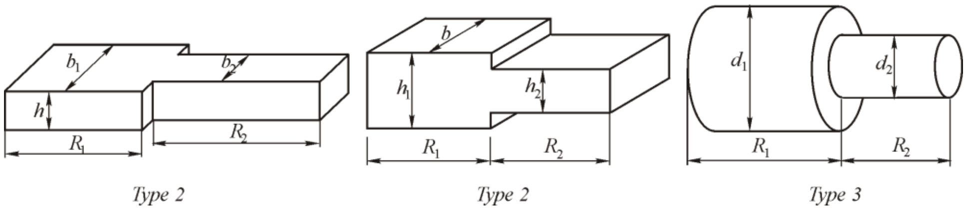

Fig. 3 Three types of beam

Three representative types are shown in Fig. 3, where ‘active’ dimensions for Type 1, 2 and 3 are breadth, depth and diameter, so that:

$$\text{For Type 1,}\ \lambda_i = \frac{b_i}{b_R},\ \delta = \frac{h_R}{L}\ ,\ \mu_i = \lambda_i\ ,\ \theta_i = \lambda_i\ ,\ \delta_R = \frac{1}{12}\delta^2\ ,$$
$$\text{For Type 2,}\ \lambda_i = \frac{h_i}{b_R},\ \delta = \frac{h_R}{L}\ ,\ \mu_i = \lambda_i\ ,\ \theta_i = \lambda_i^3\ ,\ \delta_R = \frac{1}{12}\delta^2\ , \tag{27}$$
$$\text{For Type 3,}\ \lambda_i = \frac{d_i}{d_R},\ \delta = \frac{d_R}{L}\ ,\ \mu_i = \lambda_i^2\ ,\ \theta_i = \lambda_i^4\ ,\ \delta_R = \frac{1}{16}\delta^2\ ,\ i = 1\ ,\ 2.$$

Without the loss of generality, the beam with length L and the characteristic of the first beam portion, i.e., $EI_R = EI_1$ and $m_R = m_1$, is chosen as the ‘reference’ beam. This means that in all the examples $\lambda_1 = 1$, $\mu_1 = 1$ and $\theta_1 = 1$. Taking the above into account and the fact that $R_2 = 1 - R_1$, the system dimensionless parameters are λ_2, δ and R_1.

Clearly, the critical load is a function of this parameter. Our analysis shows that the critical force can be represented in the form:

$$\tau_{cr} = \tau_{cr,u}\theta_2^{k_\theta}, \tag{28}$$

where $k_\theta = k_\theta(\textit{type of beam}, \lambda_2, \delta, R_1)$ is a dimensionless critical load parameter (CLP). For the selected set of λ_2, δ and R_1, to calculate k_θ one writes $\alpha_R = 0$ in the frequency equation (25).

The roots of the frequency equation (25) are determined by an iterative procedure based on linear interpolation and proposed in [4]. This procedure is used to calculate k_θ for $\lambda_2 = 0.6$, 0.7 & 0.8, $R_1 = 0.1, 0.2,...,1$ and $\delta = 1/20$ & 1/100. Also, for the sake of comparison, we have calculated the CLP force values for $\delta = 0$ which correspond to the case of Euler-Bernoulli beam. The CLT is tabulated in Table 1 for pinned-pinned beam.

It can be observed that the values of CLP for the uniform Euler-Bernoulli beam 0 or 1, i.e. the critical force is:

$$\tau_{cr}(R_1 = 0) = \theta_2\tau_{cr,u},\quad \tau_{cr}(R_1 = 1) = \tau_{cr,u}\ , \tag{29}$$

The previous expression applies to all the types of supports. The CLP values for Timoshenko-beam are higher which means that the critical force has less value. In order to show the trend of the change in the CLP value depending on step position R_1, the CLT values for other values of R_1 with the step of 0.001 are calculated and graphically displayed.

The Fig. 4 shows the CLP dependence on changes R_1 for values $\lambda_2 = 0.8$ and $\delta = 1/20$ & 1/100 considering the influence of the beam type. It can be noticed that the CLP values are maximal for beam type 3, while for beam type 1 are minimal. For larger values of δ (greater influence of shear) in the case when the step position is near the supports, the CLP values are maximal for type 1 and minimal for type 3. The CLP dependence on changes R_1 for types 1 and 3 and value $\delta = 1/20$, considering the influence of relations λ_2, is shown in Fig. 5. For smaller values λ_2, the CLP has higher values except in the case when the step position is near the supports; then the CLP has higher values for greater values λ_2.

Table 1 CLP for pn-pn beam

R_1	type	δ	λ_2		
			0.6	0.7	0.8
0	1	20	1.0125184	1.0179287	1.0286575
		100	1.0005022	1.0007193	1.0011497
		EB	1	1	1
	2	20	1.0015053	1.0029331	1.0061206
		100	1.0000603	1.0001175	1.0002453
		EB	1	1	1
	3	20	1.0007843	1.0015284	1.0031898
		100	1.0000314	1.0000612	1.0001277
		EB	1	1	1
0.3	1	20	0.9004332	0.8963132	0.8978066
		100	0.8881282	0.8788707	0.8701333
		EB	0.887614	0.8781417	0.8689767
	2	20	0.931096	0.9173096	0.9027403
		100	0.9295037	0.9142647	0.8965305
		EB	0.9294372	0.9141376	0.8962712
	3	20	0.942686	0.9280114	0.910252
		100	0.9418468	0.9264071	0.9069895
		EB	0.9418118	0.9263402	0.9068534
0.5	1	20	0.6063826	0.5844888	0.570687
		100	0.5934776	0.5666266	0.5427583
		EB	0.5929383	0.5658802	0.541591
	2	20	0.7353931	0.6824913	0.6268342
		100	0.7333133	0.6787341	0.6196697
		EB	0.7332265	0.6785773	0.6193705
	3	20	0.7803152	0.7240699	0.6577481
		100	0.7791806	0.7220238	0.6539021
		EB	0.7791332	0.7219384	0.6537418
0.7	1	20	0.2156296	0.202338	0.198505
		100	0.2028625	0.1846704	0.1707437
		EB	0.2023291	0.1839321	0.1695835
	2	20	0.3712844	0.2909344	0.2322638
		100	0.3680207	0.2858599	0.22374
		EB	0.3678844	0.2856479	0.2233838
	3	20	0.4593584	0.3517904	0.2614351
		100	0.4573784	0.3488207	0.2567818
		EB	0.4572958	0.3486968	0.2565878
1	1	20	0.0125184	0.0179287	0.0286575
		100	0.0005022	0.0007193	0.0011497
		EB	0	0	0
	2	20	0.0041728	0.0059762	0.0095525
		100	0.0001674	0.0002398	0.0003832
		EB	0	0	0
	3	20	0.0021755	0.0031157	0.0049801
		100	0.000087	0.0001249	0.0001996
		EB	0	0	0

Table 2 CLP for cl-cl beam

R_1	type	δ	λ_2		
			0.8	0.7	0.8
0	1	20	1.0496005	1.0710373	1.1135468
		100	1.0020083	1.0028763	1.0045974
		EB	1	1	1
	2	20	1.0060004	1.0116777	1.0243335
		100	1.0002411	1.0004699	1.000981
		EB	1	1	1
	3	20	1.0031296	1.0060937	1.0127052
		100	1.0001256	1.0002448	1.000511
		EB	1	1	1
0.3	1	20	0.790734	0.817013	0.8632652
		100	0.7347316	0.7407416	0.7464902
		EB	0.7323622	0.7375177	0.7415579
	2	20	0.7203619	0.7308869	0.7564571
		100	0.7112445	0.7154073	0.7280566
		EB	0.7108618	0.7147567	0.7268615
	3	20	0.7310421	0.7198191	0.736254
		100	0.7257155	0.7107592	0.7202147
		EB	0.7254923	0.7103792	0.7195413
0.5	1	20	0.6444095	0.6400219	0.6578166
		100	0.5907593	0.5673238	0.5458978
		EB	0.5884946	0.5642562	0.5411757
	2	20	0.6820122	0.6666843	0.6408012
		100	0.6724187	0.650626	0.6114626
		EB	0.6720159	0.649951	0.6102279
	3	20	0.6807354	0.6787212	0.6520273
		100	0.6746779	0.6692922	0.635663
		EB	0.6744238	0.6688966	0.6349761
0.7	1	20	0.2989858	0.3163953	0.3576915
		100	0.2562517	0.2540968	0.2552395
		EB	0.2544512	0.2514707	0.2509195
	2	20	0.3812923	0.3147333	0.2932055
		100	0.368565	0.2960827	0.2620313
		EB	0.3680302	0.2952983	0.2607184
	3	20	0.4648444	0.3611526	0.2934004
		100	0.4566664	0.3498693	0.2770316
		EB	0.4563232	0.3493967	0.276345
1	1	20	0.0496005	0.0710373	0.1135468
		100	0.0020083	0.0028763	0.0045974
		EB	0	0	0
	2	20	0.0165335	0.0236791	0.0378489
		100	0.0006694	0.0009588	0.0015325
		EB	0	0	0
	3	20	0.0086444	0.0123804	0.019789
		100	0.0003487	0.0004994	0.0007983
		EB	0	0	0

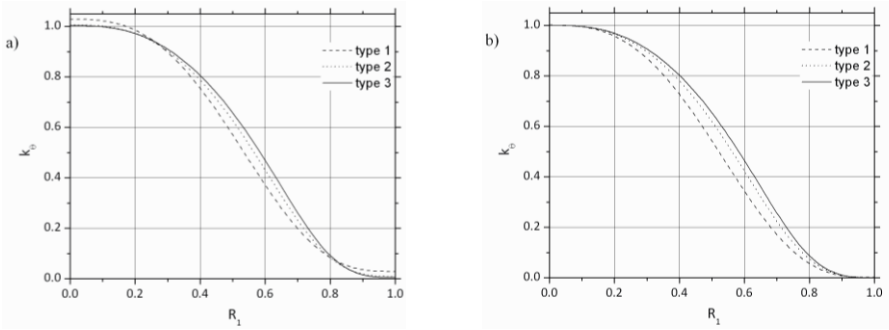

Fig 4 Variation of CLP with R_1 for pn-pn beam and $\theta_2 = 0.8$: a) $\delta = \dfrac{1}{20}$, b) $\delta = \dfrac{1}{100}$

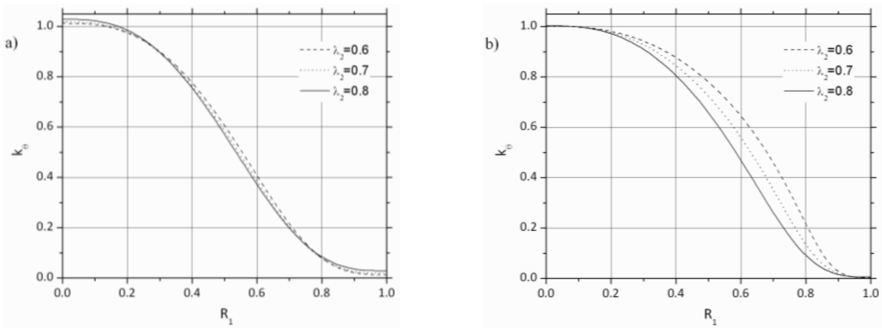

Fig 5 Variation of CLP with R_1 for pn-pn beam and $\delta = \dfrac{1}{20}$: a) type 1, b) type 3

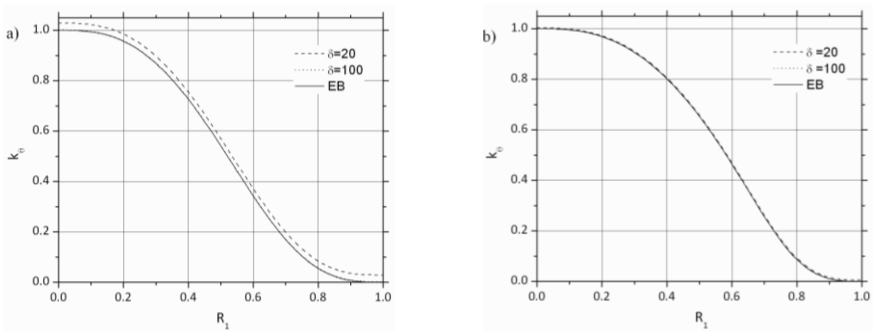

Fig. 6 Variation of CLP with R_1 for pn-pn beam and $\theta_2 = 0.8$: a) type 1, b) type 3

The CLP dependence on changes R_1 for types 1 and 3 and value $\lambda_2 = 0.8$ with influence of change values δ are shown in Fig. 6. It can be noticed that the CLP value is higher for greater values of δ. The influence of δ is higher for type 1 than for type 3.

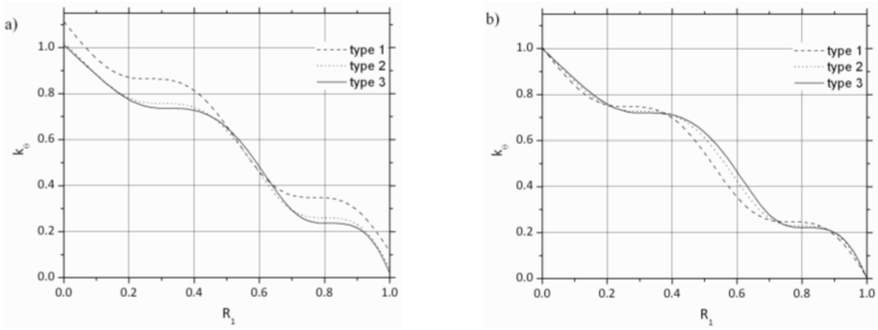

Fig. 7 Variation of CLP with R_1 for cl-cl beam and $\theta_2 = 0.8$: a) $\delta = \frac{1}{20}$, b) $\delta = \frac{1}{100}$

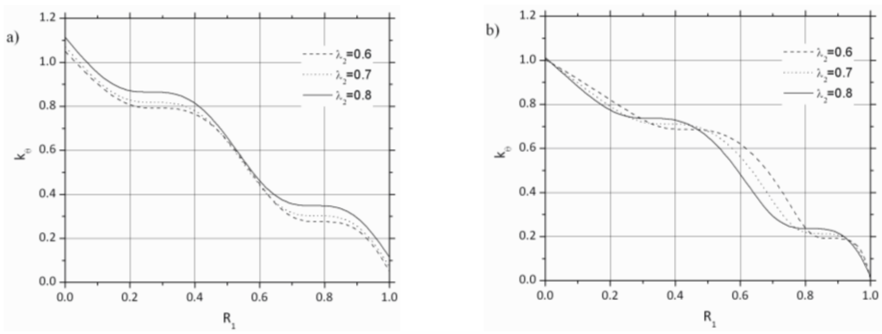

Fig. 8 Variation of CLP with R_1 for cl-cl beam and $\delta = \frac{1}{20}$: a) type 1, b) type 3

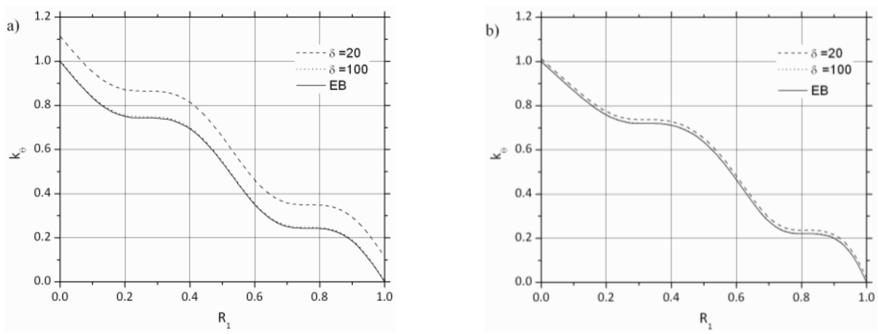

Fig. 9 Variation of CLP with R_1 for cl-cl beam and $\theta_2 = 0.8$: a) type 1, b) type 3

The CLT is tabulated as shown in Table 2 for clamped-clamped beam. In Figs.7-9, the CLP dependence on change R_1 is presented while the beam type influence, dimension ratio λ_2 and slenderness ratio δ are taken into consideration. The influence of the beam type is higher for lower values δ, as well as that of dimension ratio λ_2 for beam type 1 in relation to beam type 3. An especially large influence of slenderness ratio δ is observed for beam type 1, while for beam type 3 is considerably smaller.

Table 3 CLP for cl-fr beam

R_1	type	δ	λ_2		
			0.6	0.7	0.8
0	1	20	0.999139839	0.998768088	0.998030899
		100	0.999965631	0.999950777	0.999921322
		EB	1	1	1
	2	20	0.999896942	0.999799043	0.999580305
		100	0.999995865	0.999991949	0.999983202
		EB	1	1	1
	3	20	0.999946335	0.99989537	0.999781511
		100	0.999997843	0.999995801	0.999991243
		EB	1	1	1
0.3	1	20	0.516563665	0.493505096	0.47300968
		100	0.51772272	0.495023672	0.475235116
		EB	0.517770844	0.49508674	0.475327561
	2	20	0.652268724	0.595615643	0.5401181
		100	0.652459409	0.595956048	0.540735108
		EB	0.652467341	0.595970201	0.540760754
	3	20	0.704485327	0.640117804	0.571758088
		100	0.704588851	0.640308298	0.57210797
		EB	0.704593159	0.640316223	0.572122522
0.5	1	20	0.231981741	0.214571151	0.200117438
		100	0.233370034	0.216264853	0.202474946
		EB	0.233427646	0.216335175	0.202572866
	2	20	0.373238269	0.305011992	0.251479256
		100	0.373617013	0.305577286	0.25231405
		EB	0.373632747	0.305600765	0.252348727
	3	20	0.44925751	0.357372974	0.280582333
		100	0.449483015	0.357736179	0.281108551
		EB	0.449492388	0.357751272	0.281130422
0.7	1	20	0.055186907	0.050063457	0.045640544
		100	0.056450765	0.051615789	0.047851137
		EB	0.056503226	0.051680255	0.047942968
	2	20	0.108655097	0.079229345	0.061213511
		100	0.109305745	0.079925259	0.062080655
		EB	0.109332728	0.079954145	0.062116669
	3	20	0.156066172	0.101028811	0.07073479
		100	0.156648268	0.1015835	0.071306225
		EB	0.156672393	0.101606523	0.071329969
1	1	20	-0.00086016	-0.00123191	-0.00196910
		100	-0.00003	-0.00005	-0.00008
		EB	0	0	0
	2	20	-0.00028672	-0.00041063	-0.00065636
		100	-0.00001	-0.00002	-0.00003
		EB	0	0	0
	3	20	-0.00014906	-0.00021370	-0.00034159
		100	-0.000006	-0.000009	-0.000014
		EB	0	0	0

Table 4 CLP for cl-pn beam

R_1	type	δ	λ_2		
			0.6	0.7	0.8
0	1	20	1.025524562	1.036555975	1.058431446
		100	1.001027398	1.001471427	1.002351944
		EB	1	1	1
	2	20	1.003075743	1.005990663	1.012494595
		100	1.000123308	1.000240365	1.000501796
		EB	1	1	1
	3	20	1.001603102	1.00312319	1.006515908
		100	1.000064225	1.000125195	1.000261365
		EB	1	1	1
0.3	1	20	0.746833293	0.762347877	0.788574418
		100	0.717997588	0.723030128	0.728359103
		EB	0.716786788	0.721379896	0.72583265
	2	20	0.719999623	0.716830331	0.728191711
		100	0.715396893	0.708900445	0.713536209
		EB	0.71520442	0.708568591	0.712922479
	3	20	0.737832143	0.71734048	0.717983769
		100	0.735173101	0.712769566	0.709764639
		EB	0.735062002	0.712578473	0.709420883
0.5	1	20	0.704941873	0.707837666	0.720463214
		100	0.676340365	0.6689679	0.660927761
		EB	0.675139695	0.667336845	0.658430238
	2	20	0.681825858	0.69320834	0.696071668
		100	0.676884599	0.685081612	0.681244199
		EB	0.676677903	0.684741481	0.680623243
	3	20	0.663081249	0.684467961	0.693158972
		100	0.659887918	0.679616675	0.684818598
		EB	0.659754399	0.679413805	0.684469755
0.7	1	20	0.379309729	0.361963181	0.360261413
		100	0.35135486	0.324284617	0.302297179
		EB	0.350182851	0.322704721	0.29986644
	2	20	0.524759271	0.460060425	0.396540649
		100	0.518851854	0.450425138	0.379786092
		EB	0.518604613	0.450021642	0.37908408
	3	20	0.57511257	0.510509096	0.429191083
		100	0.571486178	0.504829574	0.419799388
		EB	0.57133452	0.504592024	0.419406539
1	1	20	0.025524562	0.036555975	0.058431446
		100	0.001027398	0.001471427	0.002351944
		EB	0	0	0
	2	20	0.008508185	0.012185324	0.019477148
		100	0.000342464	0.000490475	0.000783981
		EB	0	0	0
	3	20	0.004440154	0.006359143	0.010164521
		100	0.000178377	0.000255475	0.000408356
		EB	0	0	0

The CLT is tabulated as shown in Table 3 for clamped-free beam. Figs. 10-12 show the CLP dependence on changes R_1 while the beam type influence, dimension ratio λ_2 and slenderness ratio δ are taken into consideration. Here, the influences of parameters on the CLP values are totally clear: in the above Figs. it can be noticed that the CLP values are higher for lower values of dimension ratio λ_2, maximum for beam type 3, less for beam type 2 and minimum for beam type 1. The influence of slenderness ratio δ on the CLP values is insignificant, since the influence of shear in this manner is very small.

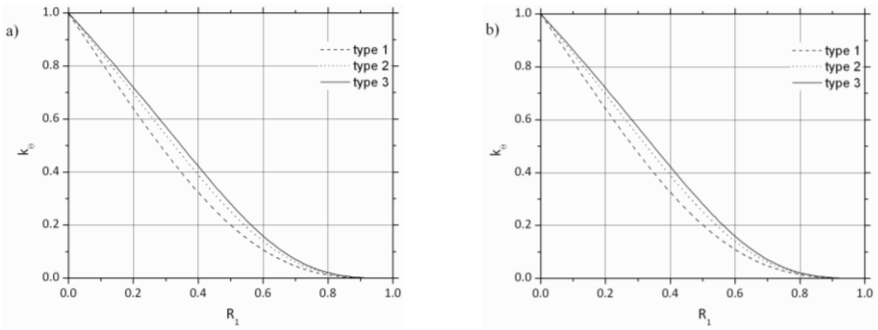

Fig. 10 Variation of CLP with R_1 for cl-fr beam and $\theta_2 = 0.8$: a) $\delta = \dfrac{1}{20}$, b) $\delta = \dfrac{1}{100}$

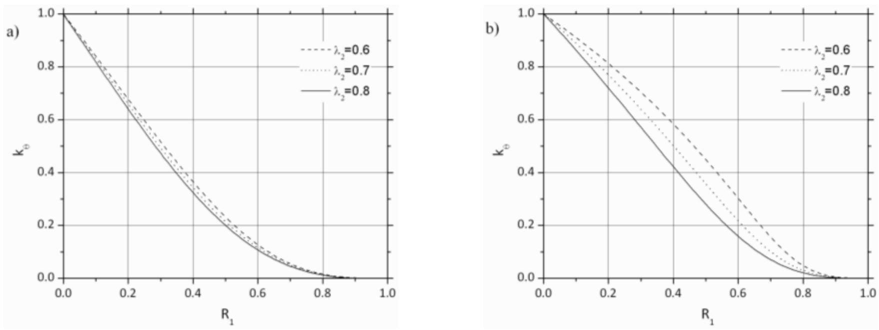

Fig. 11 Variation of CLP with R_1 for cl-fr beam and $\delta = \dfrac{1}{20}$: a) type 1, b) type 3

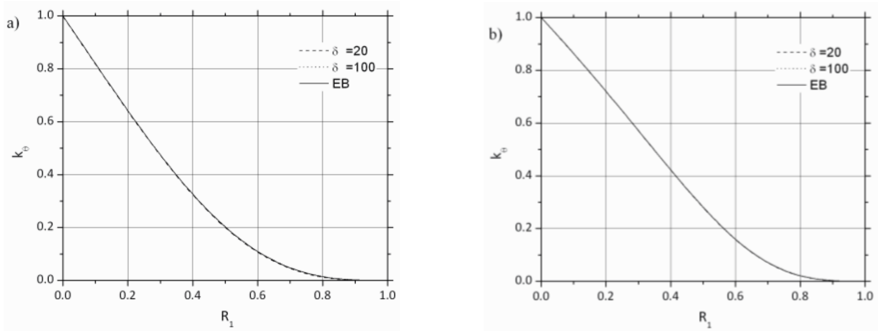

Fig. 12 Variation of CLP with R_1 for cl-fr beam and $\theta_2 = 0.8$: a) type 1, b) type 3

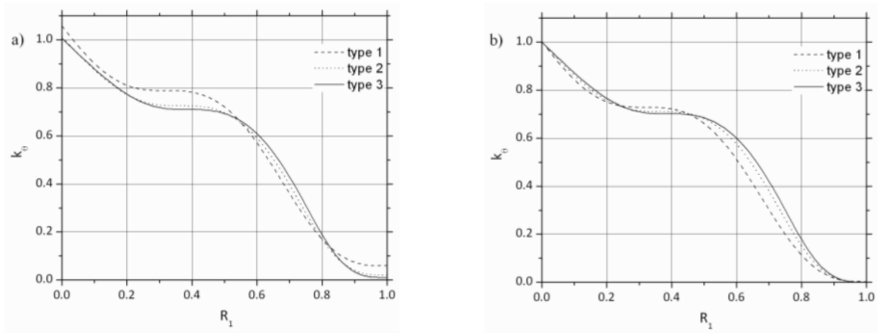

Fig. 13 Variation of CLP with R_1 for cl-pn beam and $\theta_2 = 0.8$: a) $\delta = \dfrac{1}{20}$, b) $\delta = \dfrac{1}{100}$

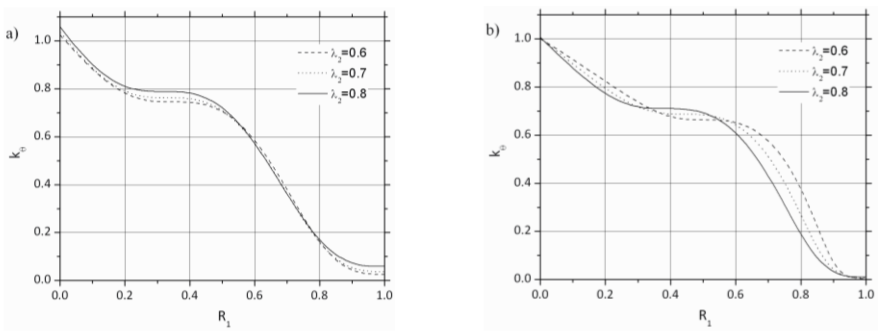

Fig. 14 Variation of CLP with R_1 for cl-pn beam and $\delta = \dfrac{1}{20}$: a) type 1, b) type 3

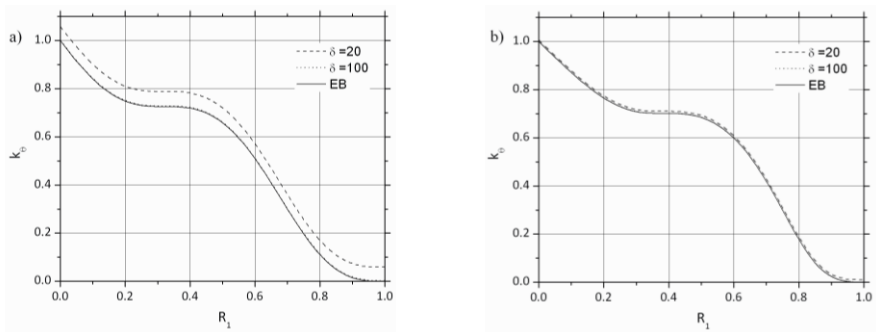

Fig. 15 Variation of CLP with R_1 for cl-pn beam and $\theta_2 = 0.8$: a) type 1, b) type 3

The CLP is tabulated as shown in Table 4 for clamped-pinned beam. In Figs.13-15, CLP dependence on change R_1 is presented while the beam type influence, dimension ratio λ_2 and slenderness ratio δ are taken into consideration. The conclusions presented in the previous cases are here confirmed, especially in the part when the step position is near the supports.

5. CONCLUSIONS

The frequency equations of one-step Timoshenko beams under compressive axial forces and four combinations of classical boundary conditions are expressed as the fourth order determinant equated to zero. The critical axial forces are expressed as a function of the critical load parameter and the critical load for uniform beam. The critical load parameters are tabulated for the beams with the classical boundary conditions. To determine the trend of change and sensibility, the dependence of the critical load parameter is displayed graphically for three types of beam in the function of step position, flexural rigidity ratio and slenderness ratio. Less sensitive are the beams with a rectangular cross-section (type 1 and type 2), while the most sensitive is the beam with a circular cross-section (type 3). Sensitivity is minor for small values of slenderness ratio due to the small influence of shear. Influence of slenderness ratio is almost nonexistent for a clamped-free beam. As far as the type of end support is concerned, there are fields with very small changes of CLP in the beams in which one of the support is clamped. Regarding a near-supports position, sensitivity is minor for pinned and free end supports and larger for a clamped end support. Also, in the beams where one of the supports is clamped there exists a field where sensitivity is very small. The method is applicable for any type of the boundary conditions and other system parameters.

REFERENCES

1. Jang, S.K., Bert, C.W., 1989, *Free vibration of stepped beams: exact and numerical solutions*, Journal of sound and vibration, 130, pp. 342-346.
2. Jang, S.K., Bert, C.W., 1989, *Free vibration of stepped beams: higher mode frequencies and effects of steps on frequency*, Journal of sound and vibration, 132, pp. 164-168.
3. Naguleswaran, A., 2006, *Vibration and stability of ring-stiffened Euler-Bernoulli tie-bars*, Applied mathematical modelling, 30, pp. 261-277.
4. Naguleswaran, A., 2004, *Transverse vibration and stability of an Euler-Bernoulli beam with step change in cross-section and in axial force*, Journal of sound and vibration, 270, pp.1045-1055.
5. Naguleswaran, A., 2003, *Vibration and stability of an Euler-Bernoulli beam with up to three-step changes in cross-section and in axial force*, International journal of mechanical sciences, 45, pp.1563-157 9.
6. Naguleswaran, A., 2002, *Natural frequencies, sensitivity and mode shape details of an Euler-Bernoulli beam with one-step change in cross-section and with endes on classical supports*, Journal of sound and vibration, 252, pp.1045-1055.
7. Naguleswaran, A., 2002, *Vibration of an Euler-Bernoulli beam on elastic end supports and with up to three step changes in cross-section*, International journal of mechanical sciences, 44 pp.2541-2555.
8. Bokaian, A., 1990, *Natural frequncies of beams under tensile axial loads*, Journal of sound and vibration, 142, pp. 481-498.
9. Bokaian, A., 1988, *Natural frequncies of beams under compressive axial loads*, Journal of sound and vibration, 126, pp. 49-65.
10. Mao, Q., 2011, *Free vibration analysis of ultiple-stepped beams by using Adomian decomposition method*, Mathematical and computer modelling, 54, pp.756-764.
11. Mao, Q., Pietrzko, S., 2010, *Free vibration analysis of stepped beams by using Adomian decomposition method*, Applied Mathematics and computation, 217, pp. 3429-3441.
12. Wu, J-S., Chang, B-H., 2013, *Free vibration of axial-loaded multi-step Timoshenko beam carrying arbitrary concentrated elements using continuous-mass transfer matrix method*, European Journal of Mechanics A/Solids, 38, pp. 20-37.
13. Zhang, Z., Huang, X., Zhang, Z., Hua, H., 2014, *On the transverse vibration of Timoshenko double-beam systems coupled with various discontinuities*, International Journal of Mechanical Sciences, 89, pp. 222-241.

KRITIČNA OPTEREĆENJE TIMOŠENKOVE STEPENASTE GREDE SA JEDNOM PROMENOM POPREČNOG PRESEKA

U radu se analiziraju transferzalne oscilacije Timošenkove grede sa jednom promenom poprečnog preseka i pritisnute aksijalnim silama koje su konstantne duž grede. Razmatrane su tri tipa grede koje se često koriste u inžinjerskoj praksi. Frekventna jednačina Timošenkove grede je prikazana u obliku determinante četvrtog reda. Kritično opterećenje je izraženo uvodjenjem parametra kritičnog opterećenja čije su vrednost iza gredu sa standardnim graničnim uslovima prikazane u tabelama. Na osnovu tih rezultata i drugih vrednosti koje su sračunate za odredjene parametre sistema, zavisnost parametra kritičnog opterećenja je prikazana grafički u funkciji položaja promene poprečnog preseka.

Ključne reči: *Timošenkova greda, frekventna jednačina, kritična sila, parametar kritičnog opterećenja, stepenasta greda.*